



ELSEVIER

Contents lists available at ScienceDirect

Journal of Magnetism and Magnetic Materials

journal homepage: www.elsevier.com/locate/jmmm

Research articles

Damping capacity, magnetic and mechanical properties of Fe-18Cr alloy

A.K. Mohamed^{a,*}, M.Yu. Zadorozhny^a, D.V. Saveliev^b, I.B. Chudakov^c, I.S. Golovin^a^a National University of Science and Technology "MISIS", Leninsky Ave. 4, 119049 Moscow, Russia^b Russian Technological University "MIREA", Pr. Vernadskogo, 78, 119454 Moscow, Russia^c I.P. Bardin Central Research Institute for Ferrous Metallurgy, 105005 Moscow, Russia

ARTICLE INFO

Keywords:

Damping capacity
Magnetostriction
High-purity materials
Fe-Cr
Magnetic properties
Spinodal decomposition

ABSTRACT

Iron-chromium based alloys are known as potentially high damping corrosion-resistance alloys with good mechanical properties and workability. The main structural mechanism of enhanced damping in the Fe-Cr alloys is magneto-mechanical coupling due to reversible and irreversible motion of magnetic domain walls, which is also linked with magnetostriction of the alloys. In order to create new complex alloyed materials with improved functional properties, it is important to study experimentally the basic relation between structure, mechanical and functional properties of binary Fe-Cr alloys. In this paper, we used cold-rolled sheets of a high-purity Fe-18Cr alloy to study the correlation between heat treatment, grain size, damping capacity and magnetostriction. Damping capacity of the samples was measured at bending using forced vibrations by means of dynamical mechanical analyzer Q800 TA Instruments and using free-decay of bending vibrations in different structural states after various annealing treatments. The results show that the optimal properties for Fe-18Cr binary alloy were achieved after annealing of cold-rolled sheets at 840 °C. Homogenizing by annealing at 1200 °C for 3 h before the final heat treatment shifts the annealing temperature for maximal damping capacity to 900 °C with approximately the same value of damping capacity and decreases mechanical properties due to the significant increase in the grain size. Slow cooling of the samples after high-temperature annealing causes a marked decrease of the impact toughness, reduction of damping capacity and an increase in the coercive force of the Fe-18Cr alloy. This effect can be explained by spinodal decomposition of the α -solid solution and formation of local zones enriched with Cr or Fe.

1. Introduction

Unwanted vibrations reduce accuracy and efficiency of sensors, laser-based information lines, optoelectronic sensors, laser gyroscopes and various optoelectronic and electromechanical devices. The vibration level in industry can be reduced using various vibro-isolating and vibro-absorbing devices based on viscoelastic organic materials [1,2]. However, viscoelastic organic materials are characterized by low elastic modulus, and application of these materials reduces rigidity of the assembly. Also, organic materials cannot be used at elevated (higher than 200 °C) or low (less than -70 °C) temperatures, for instance in the satellite systems, where a small vibration of the laser beam makes the system useless.

It is well-known that vibration, acoustic and operating properties of various precision devices can be improved with the help of High Damping Metals (HIDAMETs) [3,4]. In contrast with viscoelastic and organic materials, HIDAMETs can be characterized by high elastic modulus, good mechanical properties and high damping capacity [5].

HIDAMETs elastic modulus is comparable with the modulus E of steels and structural alloys. Several HIDAMETs, dependently on acting mechanisms of damping [6–8], can be used in a wide temperature range. For example, it has been shown [9] that vibration of the focused antenna of the Voyager long-range spacecraft was reduced using HIDAMET provided by the Proteus Company. To reduce the vibration level, lightweight precision sensors and laser devices can be attached to vibrating basements using thin-walled vibro-isolating and vibro-absorbing bearings made from the HIDAMET. In this case, the combination of desired rigidity and workability in the wide temperature range is guaranteed. However, the properties of HIDAMETs in the shape of cold-rolled (CR) thin-walled strips are not well-studied compared with thicker metallic damping materials. It is important that for this type of application, thin-walled HIDAMETs should be characterized by high corrosion resistance.

Damping capacity index ($\Psi_{01\sigma} = \Delta W/W$, where W is the maximum elastic stored energy in one cycle and ΔW is the energy absorption in that cycle's free decay damping test under stress equal to 0.1 of yield

* Corresponding author.

E-mail address: abdelkarim.abdelkarim@feng.bu.edu.eg (A.K. Mohamed).<https://doi.org/10.1016/j.jmmm.2019.165777>

Received 24 June 2019; Received in revised form 15 August 2019; Accepted 30 August 2019

Available online 31 August 2019

0304-8853/ © 2019 Published by Elsevier B.V.

Table 1
Chemical composition of the material studied (wt%).

Fe	Cr	C	Ni	Si	Al	Nb	Ti	S	N	P
base	18.4	0.009	0.014	0.12	0.02	< 0.01	< 0.01	0.004	0.014	< 0.01

stress) of metallic materials plotted vs yield strength, or ultimate tensile strength, is known as the Sugimoto diagram [10]. High-purity Fe-Cr alloys containing 14–19%Cr are characterized by enhanced specific damping capacity ($\Psi_{01\sigma/\rho}$, where ρ is density) [11]. Magnetomechanical type damping is responsible for high level damping in these alloys. Consequently, these alloys demonstrate enhanced damping capacity in the wide temperature range from liquid helium temperatures up to ~ 500 °C. According to [11–14], major contribution to the high level of damping in these alloys is connected with the irreversible movement of magnetic domain walls in the field of external elastic stresses applied to the material. It has been found [11,15,16] that damping capacity of Fe-Cr alloys is very high but it is sensitive to small modifications in the crystalline and magnetic domain structures. The Fe-Cr alloys, therefore, have good potential for new applications and can be considered as very attractive objects for investigation.

Earlier, Fe-Cr alloys were well-studied in two basic states: in the high-damping state obtained using high-temperature annealing, and in the state with suppressed damping capacity obtained, for example, using material quenching or cold rolling [16–18]. Information concerning various properties of these alloys in intermediate states (obtained using annealing at temperatures below 800–850 °C) is quite limited in the literature. However, detailed knowledge about modification of material properties in the intermediate states is very important for the development of models. Those models describe the process of formation of high-damping state in high-purity ferromagnetic alloys based on the Fe-Cr system.

Fe-Cr alloy containing 18%Cr can be considered as a model for damping alloy based on this system because of its high sensitivity of damping properties to small variations of the heat treatment temperature and the cooling rate and, consequently, to small variations in the crystalline structure [11,12]. Initial state with low damping capacity obtained using cold rolling can be easily achieved using conventional rolling mill [13]. Very high concentration of structural defects in the CR sheets provides the opportunity to form various intermediate structural states using low-temperature or high-temperature annealing. Wide variety of intermediate states exhibiting differences in the crystalline structure, mechanical, magnetic, magnetostriction and damping properties formed using various heat treatment procedures allows obtaining valuable knowledge concerning the formation of the high-damping state in Fe-Cr alloys. The above background allows formulation of the problem and local goals to be solved in the present research.

The aim of this paper is to explore the influence of annealing regimes on damping, magnetic, mechanical properties and structure of high-purity CR binary Fe-18Cr alloy. In order to obtain reliable information comparable with literature data and suitable for effective analysis, wide set of modern experimental methods studying crystalline structure, mechanical, magnetic, magnetostriction and damping properties of the material should be used for this investigation and basic principles of treatment of materials used for effective vibroisolation of precision sensors should be formulated. Obtained knowledge will be used at the next step, developing complex-alloyed materials possessing improved functional properties.

2. Experimental procedure

The studied alloy was prepared using the vacuum induction furnace “Balzers” (volume 25 kg) from high-purity raw materials. Casting was performed under argon atmosphere to produce 11 kg-ingots (2×11 kg). After machine grinding, the ingots were forged at

temperatures of 1200–1150 °C and shaped to billets with dimensions $40 \times 100 \times l$ mm. Forged billets were subjected to the machine-grinding and hot rolling at temperatures of 1200–1150 °C to obtain strips possessing thickness $t = 2.5$ mm. Strips were cleaned by pickling, followed by cold rolling from thickness of 2.5 mm to 1.0 mm using the Duo-Quattro 320 rolling mill. The range of thicknesses between $t = 0.4$ mm and $t = 1.0$ mm is typical for manufacturing vibro-absorbing supports or bearings carrying various lightweight precision sensors or vibration-sensitive devices. Chemical composition of studied alloy is presented in Table 1.

Samples for amplitude dependent internal friction (ADIF) tests were cut from a CR sheet with a thickness of 1 ± 0.05 mm. The cutting process was performed using a disc saw blade machine under high cutting speed conditions with a small feed rate and using a coolant to obtain acceptable surface quality. Samples were cut along the direction of rolling to keep deformed grains untouched. A set of heat treatments has been performed (treatment temperatures were ranged from 500 to 1000 °C) to obtain various structural states of the material.

The heat treatment regime used in the present research includes annealing in open-air or vacuum furnaces for 1hr at the specified temperatures (ranged from 500 to 1000 °C) followed by air cooling. It is important to mention that quite thick oxide films were formed on the surface of the samples after removing them from the open-air furnace (especially samples heated to a temperature higher than 800 °C). It was recently reported that cleaning the surface of the samples by grinding sand papers after heat treatment damages their damping capacity [20]. So, the samples weren't mechanically cleaned after heat treatment.

Sample sizes for measuring damping capacity under condition of free-decay oscillations are $60 \times 13 \times 1$ mm³. Samples for this test and for magnetic hysteresis loop testing were annealed using vacuum furnaces.

Homogenization by annealing in a vacuum at 1200 °C for 3hrs followed by furnace cooling (FC) was performed to form initial structure possessing enlarged grain-size and to eliminate the grain size effect during further heat treatment at lower temperatures. Samples in two initial states (CR and annealed at 1200 °C for 3hrs) were studied simultaneously to separate the effect of structure homogenization.

3. Methods

Complex investigation of the material properties has been performed using a set of experimental methods, including mechanical spectroscopy (MS), optical microscopy, hardness testing, mechanical properties studies, investigations using differential scanning calorimeter (DSC), vibrating sample magnetometer (VSM), magnetostriction studies and DC-magnetic properties investigation.

Mechanical spectroscopy is a simultaneous measuring of anelastic (internal friction, Q^{-1}) and elastic (Young's modulus, E) properties. It is known that the type of vibrations and clamping is very important for soft magnetic materials with magnetomechanical damping mechanism. The results obtained under forced vibration and results obtained under condition of free-decay oscillations may exhibit marked differences for the same alloy [20]. Both experimental techniques were employed in the present study.

The first method is based on a forced bending sample by using commercial dynamical mechanical analyzer (DMA) Q800 TA Instruments at room temperature and frequency of forced vibrations of 3 Hz using single cantilever mode. Internal friction (IF) measured by this technique as $\tan \varphi (= Q^{-1})$ at forced vibration, and $\varphi =$ phase lag

between the cyclic stress applied (σ) and resulting strain (ϵ), where $\sigma = \sigma_0 \cos(\omega t)$ and $\epsilon = \epsilon_0 \cos(\omega t + \phi)$.

The second technique is free-decay vibration of the sample clamped as a rigid cantilever to the massive suspended nonmagnetic base in the bending pendulum apparatus, known also as a clamped-free vibrating reed method. The strain range of measurements is $\epsilon = \Delta l/l = (\text{from } 2 \text{ to } 130) \times 10^{-5}$ at room temperature. Internal friction values were calculated as $Q^{-1} = (1/\pi n) \times \ln(A_i/A_{i+n})$, where A_i is the amplitude of oscillation possessing number i (numbers are counting starting from $i = 1$) and n is equal to number of oscillation cycles measured.

Microstructure was analyzed by optical microscope "Olympus". Samples were mechanically grinded and polished, followed by etching in the Waterless Kalling's etchant (ASTM E 407 designation is 95 Kalling's 2) which is composed of 5 g $\text{CuCl}_2 + 100 \text{ ml HCl} + 100 \text{ ml C}_2\text{H}_5\text{OH}$. The etching processes were done by emersion into the etchant. Standard "JMicroVision" program was used to measure grain sizes. In order to avoid incorrect grain analysis, grain contours were traced manually and, after introducing the scale bar, the program calculated average grain sizes with a high accuracy.

Vickers hardness measurements was examined by Wolpert Wilson equipment. The indentation force was set to 49 N and dwell time to 15 s (HV5 method). Ten measurements were taken over the surface of the polished sample after investigating microstructure. Tensile tests were carried out using Zwick Roell machine to obtain mechanical properties. Impact toughness was studied using CR sheets possessing thickness $t = 2.0 \text{ mm}$ in accordance with the Russian standard (GOST 9454-78, sample type 4, U-notch).

Differential scanning calorimetry (DSC) experiments using a Labsys Setaram system with heating rates of 20 K/min in air atmosphere allowed us to carry out the samples thermal analysis.

Magnetization (VSM) measurement were obtained using a VSM-130 vibrating sample magnetometer with a heating rate of 6 K/min under a magnetic field of $\approx 400 \text{ kA/m}$.

Magnetic hysteresis loops were measured in the fields of 10, 30, 300 Oe, and the quasi-static test regime was used (frequency $\sim 0.1 \text{ Hz}$). Samples in the shape of thin rectangular strips were tested using Hopkinson's permeameter. All tests were performed at room temperature. All samples for magnetic properties testing were heat-treated using the vacuum furnace. The magnetic hysteresis loops were measured along the rolling direction (dimensions $15 \times 5 \times 2 \text{ mm}^3$) parallel to an external applied magnetic field by using precision foil strain-gauge sensors. Maximum magnetic field was equal to 2 kOe. In order to analyze the correlation between annealing temperature and magnetostriction (as well as between magnetostriction and ADIF), magnetostriction of thin rectangular strips ($18 \times 6 \times 1 \text{ mm}^3$) were examined.

Magnetostriction was measured using hand-made experimental setup based on a strain gauge method up to saturated magnetic field value of 35 kA/m.

4. Experimental results and discussion

4.1. Mechanical properties and average grain size

Hardness tests are often used to estimate recrystallization temperature. By increasing annealing temperature (with a fixed annealing time of 1 h), the HV remains practically constant up to $T \approx 600 \text{ }^\circ\text{C}$. With further increase in annealing temperature, the hardness decreases sharply until $T \approx 700 \text{ }^\circ\text{C}$, and then slightly decreases to reach the minimum at $T \approx 800 \text{ }^\circ\text{C}$ (Fig. 1a). So grain size examination process started after $700 \text{ }^\circ\text{C}$ (Fig. 2a), this means that the recrystallization process in the CR Fe-18Cr alloy starts at about $600\text{--}620 \text{ }^\circ\text{C}$ and ends at about $700\text{--}800 \text{ }^\circ\text{C}$ as shown in Fig. 1a.

In order to study the effect of annealing temperature on the mechanical properties, annealed samples at different temperatures were examined by means of tensile tests. By increasing the annealing

temperature, the yield and tensile strength decrease to reach values of 270 and 400 MPa, respectively, at $840 \text{ }^\circ\text{C}$ at the end of recrystallization. The tensile strength of the samples annealed at a temperature higher than the end of recrystallization slightly decreases to reach a value of 370 MPa at $1000 \text{ }^\circ\text{C}$. But the yield strength slightly increases to reach value of 300 MPa. The reason for such different behavior is assigned to the metal softening due to the structure grain growth. The yield-to-tensile ratio for CR state is equal to 0.97, and due to annealing and softening of the metal, it decreases to reach a minimum value of 0.69 at $840 \text{ }^\circ\text{C}$, i.e. at the end of recrystallization process. Grain growth also decreases the surface area for dislocation motion, so the tensile strength decreases with increasing annealing temperature. Another effect is the increase of the elongation to reach a maximum value when the sample is fully recrystallized at $880 \text{ }^\circ\text{C}$ (Fig. 1b). Further increase of the annealing temperature (up to $T = 1000 \text{ }^\circ\text{C}$) causes drastic reduction of the relative elongation of the material (Fig. 1b). The most probably the elongation decreases as a result of grain growth (14%). These results show nearly the same trend as the results of Masumoto for Fe-Mo-Cr alloys [19].

Impact toughness was measured for samples annealed at $1000 \text{ }^\circ\text{C}$ for 40 mins followed by cooling using three different cooling rates: furnace cooling (FC), water quenching (WQ), and air cooling (AC). The effect of cooling rate was studied in order to find the most appropriate cooling conditions for the studied material. It was found that for the annealed samples, maximal KCU values were recorded in the samples subjected to water quenching ($\text{KCU} = 77 \text{ J/cm}^2$). In contrast, samples after furnace cooling demonstrate noticeable impact toughness reduction of the alloy ($\text{KCU} = 10 \text{ J/cm}^2$). Air cooled samples demonstrate intermediate values of impact toughness ($\text{KCU} = 42 \text{ J/cm}^2$). Strong influence of cooling rate on the impact toughness of the high-purity Fe-18Cr alloy can be explained by spinodal decomposition in the alloys subjected to different cooling rates from $1000 \text{ }^\circ\text{C}$.

Slow cooling of the samples in the furnace causes reduction of the impact toughness due to the spinodal decomposition of the solid solution in the temperature region of $550\text{--}400 \text{ }^\circ\text{C}$. The decomposition was indeed confirmed using small angle neutron scattering: it leads to formation of nano-sized zones enriched and depleted in Cr content. These zones become obstacles not only for dislocation motion (this effect is known as "Embrittlement $475 \text{ }^\circ\text{C}$ ") [21,22] but also for magnetic domain walls motion decreasing damping capacity of the alloy [23] and increasing the coercive force.

Microstructure investigation shows that all grains in a CR samples (observed before the recrystallization) were deformed. By completing the primary recrystallization at $700\text{--}720 \text{ }^\circ\text{C}$, the average recovered grain size is equal to $28 \pm 15 \mu\text{m}$. This grain size remains nearly constant until $T = 800\text{--}840 \text{ }^\circ\text{C}$ (Fig. 2a). Annealing at a temperature higher than $840 \text{ }^\circ\text{C}$ causes the grain growth. An increase in the average grain size until $T = 1000 \text{ }^\circ\text{C}$ can be well fitted by exponential function (Fig. 2a). Average grain size reaches the value of $315 \pm 15 \mu\text{m}$ after annealing at $T = 1000 \text{ }^\circ\text{C}$. It can be seen (Fig. 2c, d) that the increase of annealing temperature from $T = 900 \text{ }^\circ\text{C}$ to $T = 1000 \text{ }^\circ\text{C}$ causes drastic growth of the average grain size of the material.

Naturally, both annealing temperature and annealing time affect the grain size; it can be seen in Fig. 2a (inset). The increase in annealing time at $T = 950 \text{ }^\circ\text{C}$ leads to gradual growth of grains size. An average grain size increases rapidly to reach a value of $210 \mu\text{m}$ after 600 min of annealing. These results show that a wide set of structural states characterized by various grain sizes can be formed in the alloy using modification of the heat treatment conditions, which allows one to analyse modifications of magnetic, damping and magnetostriction properties in a wide range of structural states.

4.2. Damping capacity

Two types of equipment are used in our experiments: commercial DMA (forced bending of a sample in single and dual cantilever modes

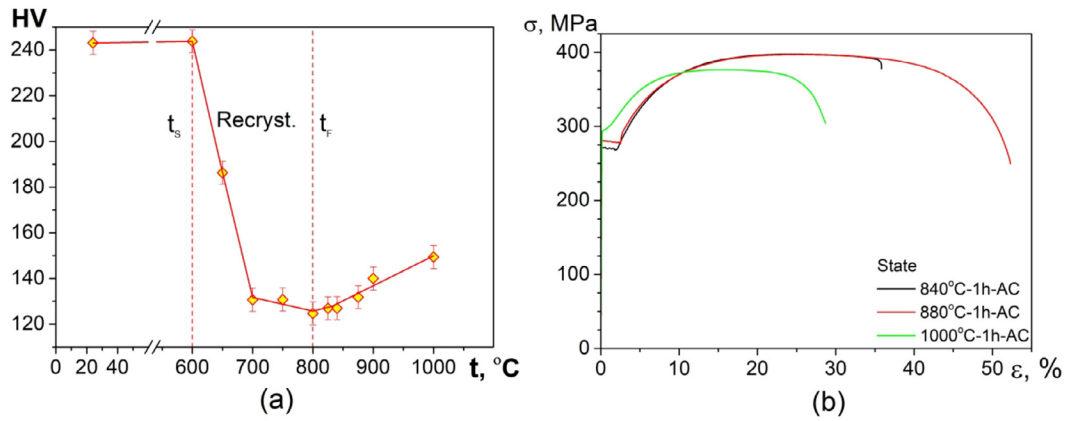


Fig. 1. Dependence of hardness on the annealing temperature (a) and stress-strain curves for samples annealed at $T = 840\text{ }^{\circ}\text{C}$, $880\text{ }^{\circ}\text{C}$ and $1000\text{ }^{\circ}\text{C}$ (b).

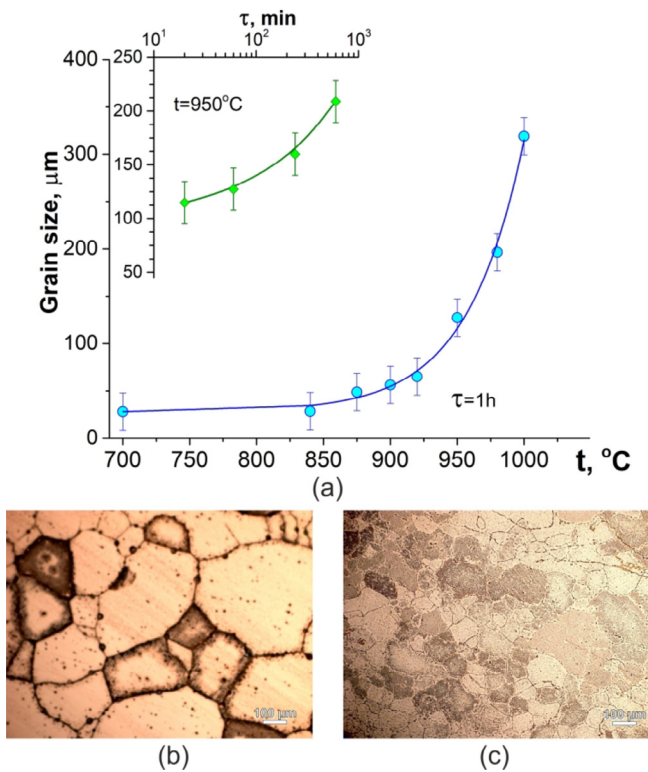


Fig. 2. Dependence of the average grain size on annealing temperature, annealing time (inset) at $T = 950\text{ }^{\circ}\text{C}$ (a) and grain structure of the alloy after annealing at $T = 1000\text{ }^{\circ}\text{C}$ for 1 hr (b) or after annealing at $T = 900\text{ }^{\circ}\text{C}$ for 1 hr (c).

with frequency $f = 3\text{ Hz}$ and bending pendulum equipment (free-decay vibrations with natural frequency of about 14 Hz). There are some systematic differences in the absolute values and position of the damping peak as well as amplitude dependent internal friction curves between these methods. Even within one type of equipment damping depends on the measuring mode. Two different modes being used for sample clamping in DMA are single and dual cantilever modes. Dual cantilever measuring mode demonstrates lower value of damping ($Q_{\max}^{-1}(\epsilon)$) compared with single cantilever mode and shifts peak values of damping to a higher strain (ϵ). The free-decay bending pendulum equipment gives higher value of (Q^{-1}) and shifts the peak to lower ϵ values. This difference originates from the static clamping stress applied to the sample. Static stresses are higher in the case of double cantilever mode as a sample is clamped in three points. It should be specially mentioned that a noticeable difference in the damping

capacity studied by two above described testing methods was observed only for materials exhibiting very high sensitivity to the application of additional static stress during IF testing [24]. HIDAMETs based on the Mn-Cu system were found to exhibit a smaller sensitivity of damping properties under additional static stress [25]. Results presented in [26] for Fe-Cr high damping alloys show nearly the same differences in the level of damping capacity between the forced vibrations mode and the free-decay mode as the results obtained in the present research.

After different annealing regimes of the CR Fe-18Cr samples, the amplitude-dependent internal friction (ADIF) curves are collected in Fig. 3: this data is achieved by using commercial DMA in a single cantilever mode. In contrast with the CR sample, ADIF curves for annealed samples exhibit a peak of magnetomechanical damping at the $Q^{-1}(\epsilon)$ curves (Fig. 3) in agreement with the theory [27] and experimental data from other researchers [12,14,27–30]. Maximal damping in the CR Fe-18%Cr alloy has been observed after 1hr annealing at $T = 840\text{ }^{\circ}\text{C}$.

The maximal damping Q_{\max}^{-1} after different annealing regimes as measured using the bending pendulum on DMA is presented in Fig. 4. In order to confirm damping level for the sample annealed at $T = 840\text{ }^{\circ}\text{C}$, several independent samples were studied for statistical reasons and the mean value of damping is presented in the Fig. 4. The absolute values of damping as measured by DMA are lower than those measured by free-decay vibrations for all heat treatment regimes.

Fig. 4 (inset plot) presents the influence of annealing time (at $T = 950\text{ }^{\circ}\text{C}$) on magnetomechanical damping (maximum Q_{\max}^{-1} value on the ADIF curve) as measured by free-decay method. Maximal damping capacity of the material has already been obtained after short-time annealing (15 min at $T = 950\text{ }^{\circ}\text{C}$). The increase of the annealing

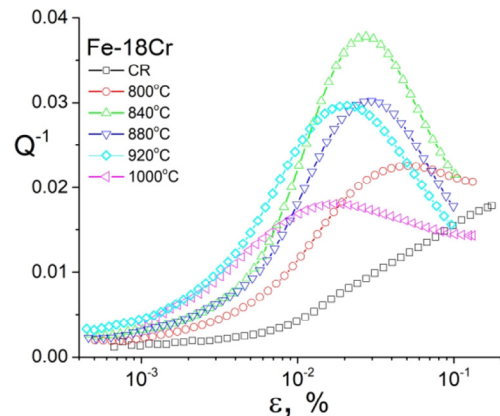


Fig. 3. ADIF measurements using commercial DMA equipment (single cantilever mode).

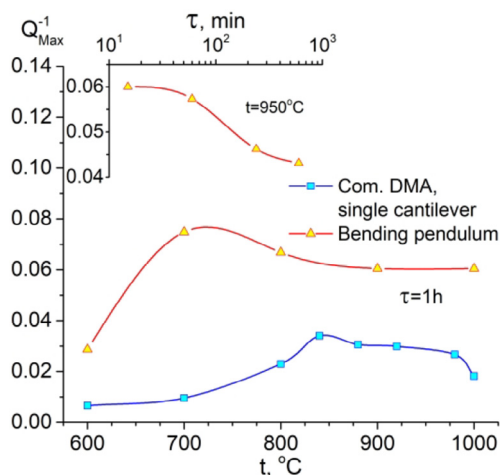


Fig. 4. Dependence of maximum damping capacity on annealing temperature and time (inset).

time causes slight decrease of the damping capacity, accompanied by marked growth of the grain size (see inset to Fig. 2, curve T = 950 °C).

In contrast with CR samples, a high level of damping capacity in hot-rolled (HR) Fe-Cr samples is recorded after annealing at 950–1000 °C for a longer time (40–60 min). The HR structure is characterized by thermally stable sub-grain microstructure with sub-grain boundaries possessing high dislocation density [31,32]. CR state is characterized by very high dislocation density as well, but it is higher and dislocations are distributed along the grain in a relatively uniform way [32]. Consequently, during annealing processes, a microstructure with low gradients of internal stresses (which is favorable for the high damping capacity) is formed much faster in the CR than in the case of the HR initial state.

Maximum damping capacity in CR high-purity Fe-18%Cr alloy is recorded after annealing at T = 750–850 °C. Further increase of the annealing temperature (up to 950–1000 °C) causes a visible decrease in the material’s damping capacity (Fig. 4). It is notable that this trend is observed for two independent measurement techniques. Experimental results, obtained earlier for Fe-16Cr-4Mo alloys [23], suggest the optimal temperature range for the formation of the highest level of damping to be 900–1000 °C. This difference can be probably explained by two reasons: first, by a high degree of cold deformation during samples rolling which provides very high dislocation density of the rolled material. The second reason is by high purity of the studied material which makes accommodation of internal stresses during annealing easier.

The effect of homogenizing the material before additional annealing at lower temperatures was investigated by pre-annealing the samples at 1200 °C for 3 h followed by furnace cooling. The IF (Q^{-1}) in the pre-annealed samples remains constant until the annealing temperature reaches T = 800 °C. Below T = 800 °C, IF of the pre-annealed samples is much higher than IF of CR materials subjected to low-temperature annealing. After annealing at T = 800–900 °C, damping capacity of the pre-annealed and CR samples is nearly the same. The increase of the temperature of additional annealing higher than T = 900 °C causes marked reduction of the IF level in the pre-annealed samples, which can be explained by excessive growth of the grain size.

4.3. Magnetic properties and magnetostriction

Magnetic properties including the cold rolled sheet curie point and the effect of cooling rate on the annealed sheet remnant magnetization and coercivity were investigated. DSC and VSM results show that the Curie point of the studied Fe-Cr alloy in the cold rolled state is equal to T ≈ 675 °C in agreement with previously reported data [33].

Magnetic hysteresis loops for the studied alloy annealed at 1000 °C and cooled down with different cooling rate are shown in Fig. 5. The

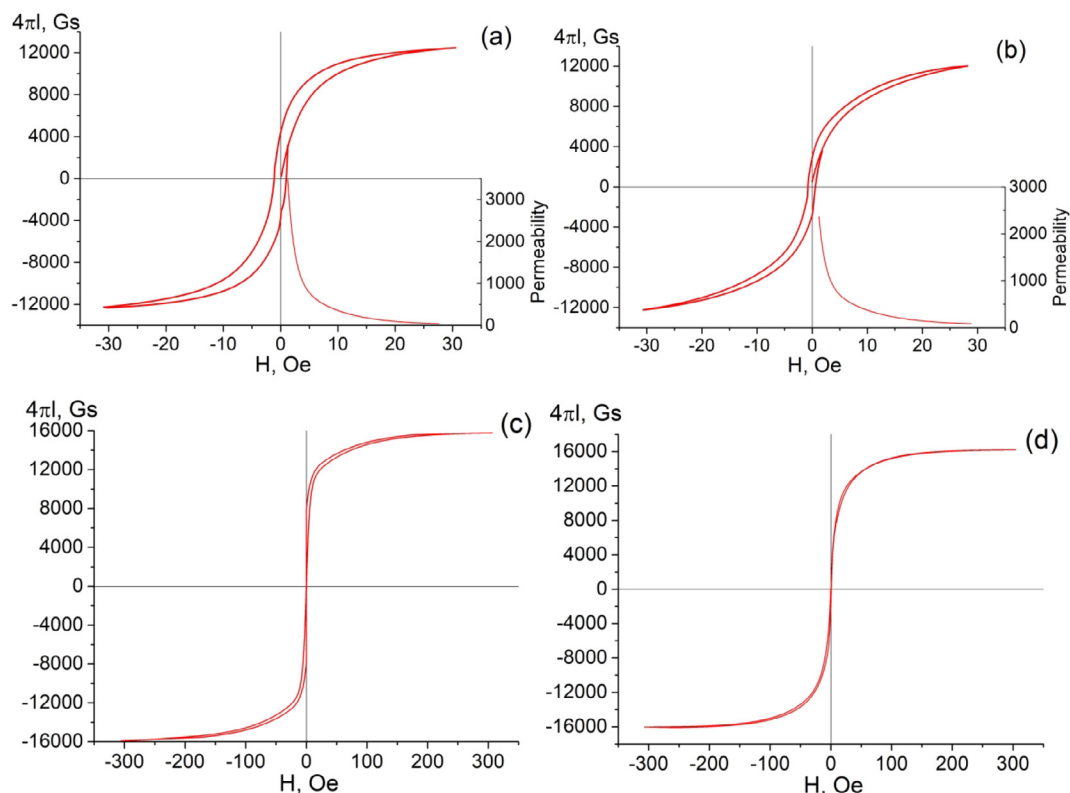


Fig. 5. Magnetic hysteresis loops for the Fe-18%Cr alloy after furnace-cooling from T = 1000 °C (a, c) and after water-quenching from 1000 °C (b, d). Hysteresis loops were recorded under maximum magnetic fields $H_{max} = 30$ Oe (a, b) and $H_{max} = 300$ Oe (c, d).

Table 2

Parameters of magnetic hysteresis loops of high-purity Fe-18Cr cold rolled alloy.

Annealed at 1000 °C followed by:	H_{max} , Oe	H_c , Oe	B_r , Gs	B_r/B_m	μ_{max}
Furnace cooling	30	0.98	4400	0.36	3300
Water quenching	30	0.65	3000	0.24	2500
Furnace cooling	300	1.18	5300	0.34	–
Water quenching	300	0.73	3300	0.20	–

change in cooling rate during heat treatment affect the shape of the magnetic hysteresis loop. The hysteresis loop consists of two regions – the first one exhibits fast increase in magnetization of the alloy under external field (the region of small magnetic fields), and the second one with the smooth growth of magnetization with applied field (Fig. 5(c, d)). The saturation magnetization in the Fe-18%Cr alloy is reached under relatively high field ($H > 300$ Oe). It indicates that the spectrum of potential barriers (hindrances) for the magnetization process are characterized by a strong energy distribution. Magnetocrystalline anisotropy of the alloy is higher in the furnace-cooled state as a result of spinodal decomposition of Fe-Cr solid solution in the furnace-cooled specimens. Magnetic hysteresis loops parameters are summarized in Table 2.

These results demonstrate the decrease of the residual magnetization level (B_r) in the water quenched sample compared with the sample after furnace cooling. The increase of the applied field from $H_{max} = 30$ Oe to $H_{max} = 300$ Oe causes a marked increase of the residual magnetization B_r for the furnace-cooled sample more than that for water quenched sample. The coercive force (H_c) of the studied alloy is much higher in the furnace-cooled state compared with the state after water-quenching (Table 2). Coercive force represents information about energy barriers which magnetic DWs overcome within one magnetization cycle. The water-quenched state is characterized by a high level of internal stresses compared with the furnace cooling, however H_c for the quenched state is lower than that is for furnace cooling (Table 2). Mentioned mismatch is the result of spinodal decomposition in the Fe-Cr alloys subjected to a slow cooling rate from $T \approx 520$ °C. These results agree with the studies of impact toughness, and it supports the choice of air-cooling of the samples during the investigation of damping capacity.

Damping capacity of HIDAMETs alloys with magnetomechanical damping mechanism is sensitive to the magnetic DWs size and shape. Longitudinal magnetostriction curves for the studied alloy in the CR state and after annealing at 840 °C and 920 °C are presented in Fig. 6 (direction of the applied magnetic field and long axis of the strain-gage were oriented along the rolling direction of the material). Magnetostriction in the annealed samples is higher compared with the CR state. The increase of annealing temperature makes the magnetostriction curve narrower up till maximum field $H \approx 200$ –250 Oe due to a decrease of internal stress level. Comparison between Figs. 5 and 6 shows that in the field of 80–350 Oe the major magnetization processes

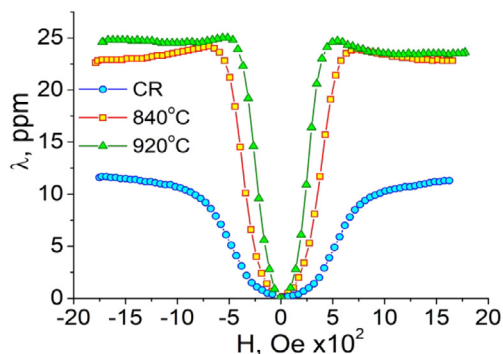


Fig. 6. Dependence of magnetostriction on the applied magnetic field.

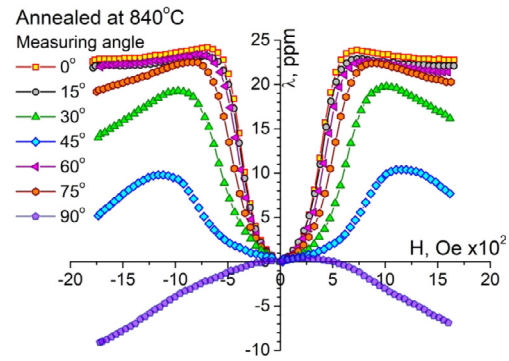


Fig. 7. Dependence of magnetostriction on the declination angle with respect to rolling direction for material annealed at 840 °C.

(displacements of the 180°-magnetic DWs) are accomplished. These values are typical for materials with relatively high magnetocrystalline anisotropy in which displacement of the 90°-magnetic domain walls occurs easier than rotation of spontaneous magnetization vectors.

Dependence of magnetostriction on the angle between the magnetic field direction and the sample's long axis (rolling direction) is presented in Fig. 7. Change of the magnetostriction curve (shape and saturation magnetostriction value) is observed for the angles from 0° to 45° between the RD and the measuring direction. Fundamental changes of magnetostriction curves appear if the angle reaches 60°. Minimum positive magnetostriction is recorded for the angle 45°, and thereafter the magnetostriction values are shifted to negative values for the angle 90°. The difference between saturation magnetostriction, measured along the RD and transversely to it, reaches 32 ppm. Strong dependence of magnetostriction on the declination angles below 45°, allows to assume that the annealing process does not change the texture in the sample although the sample annealed at a temperature higher than the recrystallization temperature.

5. Discussion

Experimental results show that various damping, mechanical and magnetic properties can be achieved in cold-rolled high-purity Fe-18%Cr alloy using various heat-treatment regimes. However, practical application of high damping alloys for anti-vibration protection of precision sensors, laser-based information lines, optoelectronic sensors, gyroscopes, various optoelectronic and electromechanical devices provides specific requirements to the combination of damping capacity, mechanical and operating properties of the material. Operating temperature should be considered when potential applicability of new material for vibro-absorbing element is analyzed in agreement with strict temperature requirements to organic vibro-absorbing elements, providing anti-vibration protection of precision sensors in currently using devices. From this viewpoint, high damping Fe-Cr alloys possess marked advantages as these materials are characterized by high level of damping capacity in a very wide temperature range from liquid helium up to $T \sim 500$ °C [23,32]. Low or high operating temperature are important for practice, e.g. in satellite systems.

High corrosion resistance of Fe-Cr alloys with $Cr > 15$ wt% is also important for vibro-isolation using thin-walled damping bearings or supports. In the same time vibro-absorbing and vibro-isolating supports carrying lightweight precision sensors should be produced from thin metallic strip in order to guarantee the combination of designed rigidity and necessary damping capacity [36]. Damping properties of materials with magnetomechanical damping mechanism are very sensitive to the application of additional static stress which decreases damping capacity of the material [25]. However, this disadvantageous special feature of Fe-Cr alloys cannot provoke serious reduction of Q^{-1} in our case because precision sensors are usually lightweight and static loading of the

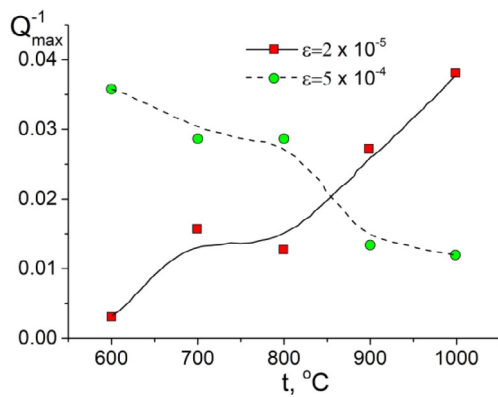


Fig. 8. Dependence of maximum damping capacity (Q_{\max}^{-1}) on annealing temperature at different strain amplitudes (free-decay vibrations of the sample).

material by weight of a sensor is negligibly small.

Possible applications of the Fe-Cr alloys as vibro-absorbing support, bearing carrying precision optoelectronic or laser devices assume different amplitude of vibrations. Three ranges of the vibration amplitude can be distinguished and analysed independently: The damping capacity in the range of very small vibration amplitudes, moderate vibrations in the intermediate amplitudes (adjacent to the peak position of damping capacity) and the damping capacity at high amplitudes, if a construction is subjected to strong vibration levels.

The values of damping capacity at low and high vibration amplitude ($\epsilon_0 = 2 \times 10^{-3}\%$ and $\epsilon_0 = 5 \times 10^{-2}\%$ respectively) as a function of the annealing temperature for the CR Fe-18%Cr alloy are represented in Fig. 8.

For low vibration amplitude, maximal damping capacity of the material is observed after annealing at a high temperature ($T = 1000^\circ\text{C}$) as shown in Fig. 8. Obtained result can be explained on the basis of the Smith and Birchak theory [34,35]: the increase of the annealing temperature causes the reduction of the internal stresses in the material and hence the increase of the damping capacity in the range of small amplitudes. It can be seen from Fig. 2 that after annealing at $T = 1000^\circ\text{C}$, the material is characterized by the highest grain size (about $320\ \mu\text{m}$). During recrystallization and increase in grain size from ~ 28 to $\sim 320\ \mu\text{m}$, the distance between the points of local pinning of magnetic domain walls reaches its maximum value. With the distance increase between the points of local DW pinning, bending of magnetic domain walls under small elastic stress takes place and the material damping capacity increases in the range of very small amplitudes. The same trend has been observed under conditions of forced vibrations – i.e. using commercial DMA instrument (see Fig. 3, $\epsilon_0 = 2 \times 10^{-3}\%$).

In contrast with the range of low vibration amplitudes, under condition of high vibrations ($\epsilon_0 = 5 \times 10^{-2}\%$), maximum values of damping capacity have been observed after annealing at $T = 600^\circ\text{C}$ as represented by the data for free-decay vibrations in Fig. 8. Annealing at 600°C gives rise to marked decrease of gradients of internal stresses in the material, so strong pinning of magnetic domain walls is no more realized. In this case in the range of high vibration amplitudes ($\epsilon_0 > 5 \times 10^{-2}\%$), marked rearrangement of the magnetic domain structure takes place under external elastic stresses and magnetic domain walls move over long distances to new pinning points, so almost all defects of the crystalline structure contribute to the overall magnetomechanical losses in the material. After annealing at low temperature, recrystallization is limited and the alloy is characterized by high concentration of structure defects, so overall losses at the high vibration amplitude are the highest.

Experimental results show that damping of high-purity cold-rolled Fe-Cr alloys can be adjusted to obtain high level of damping capacity in the field of small, intermediate or high amplitude of vibrations (Fig. 8),

so technical requirements to supports for precision sensor comply with properties of the material. Summarizing the above discussion it can be concluded that high-purity cold-rolled Fe-Cr alloys should be considered as material for manufacturing vibro-absorbing and vibro-isolating supports carrying lightweight precision sensors.

6. Conclusions

1. Enhanced damping capacity was formed in the cold rolled high-purity Fe-Cr alloys with the help of annealing heat treatment at $600\text{--}900^\circ\text{C}$. Combination of mechanical properties and damping capacity achieved in the annealed cold rolled alloys shows that this material can be used for production of lightweight vibro-absorbing and vibro-isolating pseudo-elastic elements possessing required stiffness and required damping capacity. Appropriate choice of the heat-treatment procedure allows the increase of damping capacity in the field of low vibration amplitudes ($\epsilon_0 \approx 2 \times 10^{-3}\%$), intermediate amplitudes or high vibrations ($\epsilon_0 \approx 5 \times 10^{-2}\%$), which can satisfy technical requirements for vibro-isolation of precision sensors.
2. The best damping capacity of the cold rolled Fe-18%Cr alloy was observed after annealing at $700\text{--}850^\circ\text{C}$. In contrast with damping capacity, the most significant changes in mechanical properties of the cold rolled alloy with the increase of annealing temperature took place at a lower temperature ($600\text{--}650^\circ\text{C}$). Observed difference indicates that the increase of damping capacity in the cold rolled Fe-18%Cr alloy is associated not only with the internal stresses accommodation but also with the recrystallization process.
3. Slow cooling of the samples during high-temperature heat treatment causes a marked decrease of in the impact toughness, reduction of damping capacity and increase in the coercive force of the Fe-18Cr alloy. This can be explained by spinodal decomposition of the α -solid solution accompanied by formation of local zones enriched with chromium or iron. Compared with the furnace-cooled state, quenching in water causes a decrease in the coercive force and residual magnetization in the Fe-18Cr alloy and the increase of the saturating magnetic field
4. Damping capacity of cold rolled Fe-18%Cr alloy decreases with the increase of the grain size, so annealing at a temperature higher than 900°C decreases damping capacity and provides reduction of mechanical properties of the alloy, including the yield strength and the ultimate tensile strength. Obtained results are in agreement with the trend provided by the Sugimoto plot.
5. Annealing of cold rolled samples of Fe-18%Cr alloy at $600\text{--}950^\circ\text{C}$ leads to valuable increase in longitudinal magnetostriction (more than 2.5 times compared with the cold rolled state). The enhanced magnetostriction provides a necessary condition for the activation of magnetic domain walls motion (under the field of external alternating elastic stress) and hence for the formation of high damping state.
6. At the early stage of Fe-18Cr alloy recrystallization, minimal values of the magnetostriction are observed if the declination angle ranges between 75° and 90° with respect to the rolling direction. Analysis of magnetic hysteresis loops is in agreement with the results of magnetostriction tests.

Acknowledgements

The work was carried out with support from the Ministry of Education and Science of the Russian Federation in the framework of increase Competitiveness Program of NUST “MISIS”, implemented by a governmental decree dated 16th of March 2013, No 211. This work was supported by the RNF project 19-72-20080. The authors are grateful to Dr A. Islamov for SAS neutron scattering study of Fe-18Cr annealed samples which proves their spinodal decomposition.

References

- [1] T. Claudia, N. Valentin, L. Gabriel, Actual stage of industrial noise reduction, *J. Eng. Stud. Res.* 17 (2011) 89–95.
- [2] C.H. Hansen, B.I.F. Goelzer, *Eng. Noise Control* 10 (2007) 245–296.
- [3] D.W. James, High damping metals for engineering applications, *Mater. Sci. Eng.* 4 (1969) 1–8, [https://doi.org/10.1016/0025-5416\(69\)90033-0](https://doi.org/10.1016/0025-5416(69)90033-0).
- [4] R. De Batist, High damping materials: mechanisms and applications, *J. Phys. Colloq.* 44 (1983) 39–50.
- [5] N. Igata, K. Nishiyama, K. Ota, Y. Yin, W. Wuttig, I.S. Golovin, J.V. Humbeeck, J. San Juan, Panel discussion on the application of HDM, *J. Alloys Compd.* 355 (2003) 230–240, [https://doi.org/10.1016/S0925-8388\(03\)00235-4](https://doi.org/10.1016/S0925-8388(03)00235-4).
- [6] R. De Batist, Internal Friction of Structural Defects in Crystalline Solids, North Holland Publisher Co., Amsterdam, The Netherlands, 1972.
- [7] M.S. Blanter, I.S. Golovin, H. Neuhäuser, H.-R. Sinning, Internal friction in metallic materials. A Handbook. Springer Series, *Mater. Sci.* (2007), <https://doi.org/10.1109/MCISE.2001.963423>.
- [8] I.S. Golovin, Damping mechanisms in high damping materials, *Key Eng. Mater.* 319 (2006) 225–230, <https://doi.org/10.4028/www.scientific.net/KEM.319.225>.
- [9] F. Scarpa, S. Jacobs, C. Coconnier, M. Toso, D. Di Maio, Auxetic shape memory alloy cellular structures for deployable satellite antennas: design, manufacture and testing, *EPJ Web Conf.* 6 (2010) 27001, <https://doi.org/10.1051/epjconf/20100627001>.
- [10] K. Sugimoto, High-damping alloys—a review on basic problems, *J. Jpn. Inst. Met.* 14 (1975) 491–498.
- [11] B.M. Girish, B.M. Satish, K. Mahesh, Vibration damping of high-chromium ferromagnetic steel and its dependence on magnetic domain structure, *J. Alloys Compd.* 484 (2009) 296–299, <https://doi.org/10.1016/j.jallcom.2009.04.085>.
- [12] H. Wang, F. Wang, J. Xiao, Y. Wang, C. Ma, Z. Dou, M. Wang, P. Zhang, Effect of cooling rate on damping capacity of Fe-Cr based ferromagnetic metal alloy, *Mater. Sci. Eng. A* 650 (2016) 382–388, <https://doi.org/10.1016/j.msea.2015.10.086>.
- [13] H. Wang, F. Wang, H. Liu, D. Pan, Q. Pan, Y. Liu, J. Xiao, P. Zhang, Influence of alloy elements (Mo, Nb, Ti) on the strength and damping capacity of Fe-Cr based alloy, *Mater. Sci. Eng. A* 667 (2016) 326–331, <https://doi.org/10.1016/j.msea.2016.05.013>.
- [14] L. Duan, D. Pan, H. Wang, J. Wang, Investigation of the effect of alloying elements on damping capacity and magnetic domain structure of Fe-Cr-Al based vibration damping alloys, *J. Alloys Compd.* 695 (2017) 1547–1554, <https://doi.org/10.1016/j.jallcom.2016.10.297>.
- [15] X. Hu, Y. Du, D. Yan, L. Rong, Effect of Cu content on microstructure and properties of Fe-16Cr-2.5Mo damping alloy, *J. Mater. Sci. Technol.* 34 (2018) 774–781, <https://doi.org/10.1016/j.jmst.2017.05.007>.
- [16] R.M. Bozorth, R.M.B. Magnetic, J.P. Radium, Magnetic domain patterns, *J. Phys. Le Radium.* 12 (1951) 308–321.
- [17] W. Wang, B. Zhou, The correlation of damping capacity with grain-boundary precipitates in Fe-Cr-based damping alloys annealed at high temperature, *Mater. Sci. Eng. A* 366 (2004) 45–49, <https://doi.org/10.1016/j.msea.2003.08.065>.
- [18] Y. Xu, L. Ning, Y. Wen, Effect of domain variations on damping capacity of Fe – 16Cr – 2.5Mo alloy solution annealed at 1373 K and 1473 K, *J. Magn. Magn. Mater.* 323 (2011) 819–821, <https://doi.org/10.1016/j.jmmm.2010.11.023>.
- [19] B.H. Masumoto, M. Hinai, S. Sawaya, Damping capacity and pitting corrosion resistance of Fe-Mo-Cr alloys, *Trans. Japan Inst. Met.* 27 (1986) 401–407.
- [20] A. Emdadi, M.A. Nartey, Y.G. Xu, I.S. Golovin, Study of damping capacity of Fe-5.4Al-0.05Ti alloy, *J. Alloys Compd.* 653 (2015) 460–467, <https://doi.org/10.1016/j.jallcom.2015.09.031>.
- [21] I.S. Golovin, V.I. Sarrak, S.O. Suvorova, Influence of carbon and nitrogen on solid solution decay, *Metall. Trans. A* 23 (1992) 2567–2579, <https://doi.org/10.1007/BF02658060>.
- [22] D. Chen, A. Kimura, W. Han, Correlation of Fe/Cr phase decomposition process and age-hardening in Fe-15Cr ferritic alloys, *J. Nucl. Mater.* 455 (2014) 436–439, <https://doi.org/10.1016/j.jnucmat.2014.07.069>.
- [23] I.S. Golovin, Mechanism of damping capacity of high-chromium steels and α -Fe and its dependence on some external factors, *Metall. Mater. Trans. A* 25 (1994) 111–124.
- [24] F. Yin, S. Takamori, Y. Ohsawa, A. Sato, K. Kawahara, The effects of static strain on the damping capacity of high damping alloys, *Mater. Trans.* 43 (2002) 466–469, <https://doi.org/10.2320/matertrans.43.466>.
- [25] I.B. Chudakov, N.M. Aleksandrova, S.Y. Makushev, T.A. Turmambekov, Influence of plastic deformation and asymmetric loading on the properties of Fe-Al and Mn-Cu damping alloys, *Steel Transl.* 47 (2017) 428–433, <https://doi.org/10.3103/S0967091217060031>.
- [26] F.X. Yin, X.Y. Li, X.F. Hu, S.W. Liu, Y.Y. Li, B. Zhang, L.J. Rong, Influence of static stress on damping behavior in Fe-15Cr and Fe-8Al ferromagnetic alloys, *Mater. Sci. Eng. A* 528 (2011) 5491–5495, <https://doi.org/10.1016/j.msea.2011.03.062>.
- [27] V.F. Coronel, D.N. Beshers, Magnetomechanical damping in iron, *J. Appl. Phys.* 64 (1988) 2006–2015, <https://doi.org/10.1063/1.341757>.
- [28] Y.G. Xu, X.G. Chen, On relationship between annealing treatment and magnetostriiction behavior of Fe-16Cr-2.5Mo damping alloy, *J. Alloys Compd.* 582 (2014) 364–368, <https://doi.org/10.1016/j.jallcom.2013.08.070>.
- [29] H. Wang, W. Li, T. Hao, W. Jiang, Q. Fang, X. Wang, T. Zhang, J. Zhang, K. Wang, L. Wang, Mechanical property and damping capacity of ultrafine-grained Fe-13Cr-2Al-1Si alloy produced by equal channel angular pressing, *Mater. Sci. Eng. A* 695 (2017) 193–198, <https://doi.org/10.1016/j.msea.2017.04.018>.
- [30] I.S. Golovin, N.Y. Rokhmanov, Question of the mechanism of formation of the damping condition of high-chromium ferritic steels, *Met. Sci. Heat Treat.* 35 (1993) 526–533, <https://doi.org/10.1007/BF00774921>.
- [31] V.A. Udovenko, I.B. Chudakov, N.A. Polyakova, The fine crystalline and magnetic structure of high-damping alloys based on the Fe-Cr system, *Phys. Met. Met.* 75 (1993) 247–251.
- [32] I.B. Chudakov, I.S. Golovin, Effect of crystalline and magnetic structure on magnetomechanical damping of Fe-Cr based alloys, in: V. Kinra (Ed.), *M3D III, Mech. Mech. Mater. Damping*, ASTM STP 1304, Philadelphia, 1997, pp. 162–178.
- [33] O. Kubaschewski, Iron—Chromium Fe—Cr, *IRON—Binary Phase Diagrams*, Springer Berlin Heidelberg, Berlin, Heidelberg, 1982, pp. 31–34, https://doi.org/10.1007/978-3-662-08024-5_17.
- [34] G.W. Smith, J.R. Birchak, Effect of internal stress distribution on magnetomechanical damping, *J. Appl. Phys.* 39 (1968) 2311–2316, <https://doi.org/10.1063/1.1656551>.
- [35] G.W. Smith, Internal stress distribution theory of magnetomechanical hysteresis—an extension to include effects of magnetic field and applied stress, *J. Appl. Phys.* 40 (1969) 5174, <https://doi.org/10.1063/1.1657370>.
- [36] Hosoya Takeshi, “Vibration isolation device using damping alloy,” Japanese Patent No JP2012037039 (A), 2012-02-23.